



Flotillins in the intercalated disc are potential modulators of cardiac excitability



Elise L. Kessler^{a,*}, Leonie van Stuijvenberg^a, Joanne J.A. van Bavel^a, Joëlle van Bennekom^a, Anne Zwartsen^{b,c}, Mathilde R. Rivaud^a, Aryan Vink^d, Igor R. Efimov^e, Alex V. Postma^f, J. Peter van Tintelen^{f,g}, Carol A. Remme^h, Marc A. Vos^a, Antje Banningⁱ, Teun P. de Boer^a, Ritva Tikkanenⁱ, Toon A.B. van Veen^a

^a Department of Medical Physiology, Division of Heart & Lungs, University Medical Center Utrecht, Utrecht, the Netherlands

^b Dutch Poisons Information Center (DPIC), University Medical Center Utrecht, Utrecht University, Utrecht, the Netherlands

^c Neurotoxicology Research Group, Division Toxicology, Institute for Risk Assessment Sciences (IRAS), Faculty of Veterinary Medicine, Utrecht University, Utrecht, the Netherlands

^d Department of Pathology, University Medical Center Utrecht, Utrecht, the Netherlands

^e Department of Biomedical Engineering, George Washington University, Washington, DC, USA

^f Department of Clinical Genetics, Amsterdam University Medical Center, Location AMC, the Netherlands

^g Department of Genetics, University Medical Center Utrecht, Utrecht, the Netherlands

^h Department of Clinical and Experimental Cardiology, Academic Medical Center, University of Amsterdam, the Netherlands

ⁱ Institute of Biochemistry, Medical Faculty, University of Giessen, Germany

ARTICLE INFO

Keywords:

Flotillin
Reggie
Desmosome
Intercalated disc
Cardiac excitation
Na_v1.5

ABSTRACT

Background: The intercalated disc (ID) is important for cardiac remodeling and has become a subject of intensive research efforts. However, as yet the composition of the ID has still not been conclusively resolved and the role of many proteins identified in the ID, like Flotillin-2, is often unknown. The Flotillin proteins are known to be involved in the stabilization of cadherins and desmosomes in the epidermis and upon cancer development. However, their role in the heart has so far not been investigated. Therefore, in this study, we aimed at identifying the role of Flotillin-1 and Flotillin-2 in the cardiac ID.

Methods: Location of Flotillins in human and murine cardiac tissue was evaluated by fluorescent immunolabeling and co-immunoprecipitation. In addition, the effect of Flotillin knockout (KO) on proteins of the ID and in electrical excitation and conduction was investigated in cardiac samples of wildtype (WT), Flotillin-1 KO, Flotillin-2 KO and Flotillin-1/2 double KO mice. Consequences of Flotillin knockdown (KD) on cardiac function were studied (patch clamp and Multi Electrode Array (MEA)) in neonatal rat cardiomyocytes (NRCMs) transfected with siRNAs against Flotillin-1 and/or Flotillin-2.

Results: First, we confirmed presence in the ID and mutual binding of Flotillin-1 and Flotillin-2 in murine and human cardiac tissue. Flotillin KO mice did not show cardiac fibrosis, nor hypertrophy or changes in expression of the desmosomal ID proteins. However, protein expression of the cardiac sodium channel Na_v1.5 was significantly decreased in Flotillin-1 and Flotillin-1/2 KO mice compared to WT mice. In addition, sodium current density showed a significant decrease upon Flotillin-1/2 KD in NRCMs as compared to scrambled siRNA-transfected NRCMs. MEA recordings of Flotillin-2 KD NRCM cultures showed a significantly decreased spike amplitude and a tendency of a reduced spike slope when compared to control and scrambled siRNA-transfected cultures.

Conclusions: In this study, we demonstrate the presence of Flotillin-1, in addition to Flotillin-2 in the cardiac ID. Our findings indicate a modulatory role of Flotillins on Na_v1.5 expression at the ID, with potential consequences for cardiac excitation.

* Corresponding author at: Department of Medical Physiology, Division of Heart & Lungs, University Medical Center Utrecht, Yalelaan 50, 3584CM Utrecht, the Netherlands

E-mail address: e.l.kessler@umcutrecht.nl (E.L. Kessler).

<https://doi.org/10.1016/j.yjmcc.2018.11.007>

Received 12 July 2018; Received in revised form 12 November 2018; Accepted 13 November 2018

Available online 17 November 2018

0022-2828/ © 2018 Elsevier Ltd. All rights reserved.

1. Introduction

Maladaptive cardiac remodeling, compromised propagation of the electrical impulse and heart disease are often associated with alterations in the intercalated disc (ID), which is the mechanical and electrical contact region between adjacent cardiomyocytes [1]. The major structures in the ID are gap junctions, adherens junctions, desmosomes and ion channels [2]. Gap junctions enable the electrical coupling between cardiomyocytes and allow small molecules to pass from one cytosol to the other. The main gap junction protein in the ventricles is Connexin-43 (Cx43) [3]. Adherens junctions and desmosomes are responsible for the mechanical coupling, connecting actin filaments of adjacent cardiomyocytes and linking the cell to the intermediate filaments, respectively. Ion channels, such as the sodium channel $\text{Na}_v1.5$, enable excitation of the cardiomyocytes [4].

Despite the accumulating knowledge of the ID, its exact content and composition is not yet fully understood. Recently, a proteomics study, in which enriched cardiac membrane fractions were analyzed and the obtained data were subjected to system biology approaches, revealed various proteins to be present in the cardiac ID. For many of those proteins, the precise location and function in the heart were thus far unknown. One of these proteins was Flotillin-2, for which the localization at the ID was confirmed by immunohistochemical staining of human, murine, rat and canine cardiac tissue sections. Moreover, Flotillin-2 in the ID was suggested to be increased in patients with Arrhythmogenic Cardiomyopathy (ACM) and Dilated Cardiomyopathy (DCM), as compared to control specimens, thereby proposing a role in cardiac remodeling during disease [5].

The Flotillin protein family consists of Flotillin-1/Reggie-2 and Flotillin-2/Reggie-1. Flotillins are highly conserved among species and expressed in almost all vertebrate cell types [6–8]. Both Flotillins are homologous proteins with an amino acid sequence identity of about 50%. The proteins consist of two parts: the N-terminus that mainly regulates their membrane interaction and the C-terminus that is responsible for oligomerization and most protein interactions known so far [9]. In general, Flotillin-2 is predominantly detected at the cell membranes. Although it does not contain a transmembrane domain, it is associated with the membrane by means of myristoylation and palmitoylation [7,10,11]. Due to lack of myristoylation and only a single palmitoylation site, Flotillin-1 is a more soluble protein and next to the cell membrane also present in intracellular organelles like the nucleus and the Golgi complex [10,12–14]. At the plasma membrane, Flotillins co-assemble and form stable clusters, distributed over the cell-cell contacts of most cells [7,15]. After hetero-oligomerization, Flotillins can translocate to intracellular compartments, where Flotillin-2 has been reported to stabilize Flotillin-1 [16–18]. Short interfering RNA mediated decrease of Flotillins therefore also results in a reduction of the other Flotillin, and Flotillin-2 KO or depletion in cells also seems to induce degradation of Flotillin-1, suggesting redundancy or dependency between the family members. [16,19,20]

Although Flotillins are known to play a role in various cellular processes, such as e.g. cell-cell and cell-matrix adhesion, and membrane trafficking, their behavior in the heart has not yet been thoroughly studied [14,19–25]. Remarkably, despite the evidence for the importance of Flotillins in many cellular processes, Flotillin-1, Flotillin-2 and Flotillin1/2 KO mice are viable and global KO in all cell types does not show a major phenotype [26].

In the context of pathophysiology, Flotillins are primarily known for their role in cancer where they promote tumorigenesis and metastasis [27–31], while Flotillin-2 deficiency in turn causes a reduction in tumorigenicity and e.g. lung metastases [32].

Interestingly, as discovered in cancer research, expression of Flotillins seems to be important for the formation, organization and stabilization of adherens junctions and desmosomes [23,33,34]. Flotillins are able to co-immunoprecipitate with N-Cadherin (Ncad), α -Catenin, β -Catenin, E-Cadherin, Plakoglobin and Desmoglein (DSG)

[20,23,34,35]. Flotillin knockdown (KD) in epidermoid carcinoma cells appears to regulate E-Cadherin recycling, and results in weakening of the desmosomal adhesion [20,23,34]. However, it is not known if these interactions also take place in cardiac tissue, and the influence of Flotillins on other components of the ID or on cardiac excitation and conduction has not yet been studied.

In the present study, we aimed at identifying the role of Flotillin-1 and Flotillin-2 in the heart. We therefore studied their presence in human cardiac specimen and investigated their relationship to the ID. We specially focused on the potential relationship of Flotillins with functionality of desmosomal and adherens junction proteins, but also with the gap junction protein Cx43 and the sodium channel $\text{Na}_v1.5$. Furthermore, we used a knockout (KO) mouse model and cultured neonatal rat cardiomyocytes (NRCMs) treated with siRNAs to explore potential consequences of Flotillin deficiency for cardiac remodeling, excitation and conduction.

2. Material & methods

To investigate the role of Flotillin-1 and Flotillin-2 in the heart, different models were used: 1) Human left ventricular cardiac tissue from one healthy control and one patient with ACM 2) Hearts from wildtype (WT) mice, Flotillin-1 KO, Flotillin-2 KO and Flotillin-1/2 KO mice, and 3) Ventricular NRCMs, which were either untreated (control) or transfected with a scrambled siRNA (scrambled), siRNA against Flotillin-1 (Flotillin-1 KD), siRNA against Flotillin-2 (Flotillin-2 KD) or both siRNAs (Flotillin-1/2 KD).

2.1. Origin of material and ethical statements

The study met the criteria of the code of proper use of human tissue that is used in the Netherlands. Human cardiac specimens were obtained from the Cardiac tissue bank of the Department of Pathology, University Medical Center Utrecht, the Netherlands. The procedure of obtaining human samples was approved by the scientific advisory board of the biobank of the University Medical Center Utrecht (protocol no. 12/387).

Genetically engineered Flotillin-2 KO mice were generated as described by Banning et al. [27]. Briefly, exon one was deleted using a Cre-Lox-system and KO was confirmed by Southern Blot. Flotillin-1 KO mice were published in Ludwig et al. [36]. Flotillin-1/2 double KO mice were created by cross-breeding of the single KO mice. All procedures with laboratory animals used in this study have been declared to the Animal Welfare Office of the Justus-Liebig-University Giessen (registry number 575_M). The mice were treated in strict accordance with the recommendations of the Guide for the Care and Use of Laboratory Animals of the National Institutes of Health and of local authorities. All animals were sacrificed by cervical dislocation after deep isoflurane anesthesia to ensure minimal suffering. After sacrifice hearts were snap frozen in liquid nitrogen and stored at -80°C . Male and female mice from the following groups were used for experiments and analyses: WT mice ($n = 9$, age 5.1 ± 0.1 months), Flotillin-1 KO mice ($n = 7$, age 5.4 ± 0.1 months), Flotillin-2 KO mice ($n = 6$, age 4.9 ± 0.6 months) and Flotillin-1/2 KO mice ($n = 8$, age 4.8 ± 0.1 months).

For the isolation of NRCMs, pregnant Wistar RCC rats were purchased from Envigo, The Netherlands. Experiments on neonatal rats were conducted with consent of the Experimental Animal Ethics Committee of the Utrecht University, the Netherlands.

2.2. Isolation of ventricular neonatal rat cardiomyocytes

NRCMs were isolated from hearts of 1- to 2-day old Wistar rats. Neonatal rats were sacrificed by decapitation, hearts were excised aseptically, and vessels and atria were removed. Ventricles were washed in Solution A (Hanks' Buffered Salt Solution-based medium) and minced into small pieces of $\pm 2\text{mm}^3$. Tissue pieces were then

transferred into a sterile glass bottle containing 14 mL Solution-A supplemented with 2.5% Trypsin (Gibco by Life Technologies, Breda, The Netherlands) and 10 µg/mL DNase (Gibco), and shaken in a water bath set to 37 °C for 15 min. Next, the solution was mixed by pipetting up and down and the supernatant was transferred into a sterile 50 mL tube. Fresh enzyme solution was added to the sediment and again shaken for 15 min. The tube containing supernatant was centrifuged for 3 min at 1100 rpm without brake, supernatant was discarded, and the pellet was dissolved in Ham's F10 medium (Thermo Fisher Scientific, Breda, The Netherlands) without calcium and magnesium. This was repeated 4–5 times until all tissue pieces were dissolved and all supernatants were collected.

To remove cell debris, cells were filtered and pre-plated in uncoated culture dishes for 2 h to enrich the myocyte population, and to remove fibroblasts and other non-cardiomyocytes. Afterwards, cells were collected by centrifugation for 3 min at 1100 rpm with brake, and 10 mL fresh Hams' F10 supplemented with 5% fetal calf serum (Lonza, Verviers, Belgium), penicillin/streptomycin (Lonza) and L-Glutamine (Lonza) was added. Then, cells were counted and cultured on laminin-coated (Roche, Mannheim, Germany) cell culture dishes at a density of 250.000 cells/cm² for Western Blotting, on transparent Multi Electrode Array (MEA) plates (Axion Biosystems Inc., Atlanta, USA) at a density of 1.15×10^5 cells/cm² to create a monolayer, or at a density of 12.500 cells/cm² for patch clamp. Twenty-four hours after plating, medium was changed.

2.3. Fluorescent immunolabeling

Immunolabeling of 10 µm thick human or murine four-chamber-view cryo sections was performed as described previously [37], using mouse monoclonal antibodies against pan-cadherin (1:800, Sigma-Aldrich, St. Louis, USA) and Cx43 (1:250, BD Transduction Laboratories, Breda, The Netherlands), and rabbit polyclonal antibodies against Flotillin-1 (1:100, Sigma-Aldrich). Secondary labeling was achieved by appropriate fluorescein isothiocyanate (FITC, 1:250) or Alexa Fluor 594 (1:100) conjugated anti-mouse or anti-rabbit whole IgG antibodies (Jackson ImmunoResearch Europe, Newmarket, United Kingdom). Pictures were taken using a Leica SP8 X white light laser confocal microscope and a 63× objective with or without digital zoom and the Leica Software LAS X.

2.4. Immunoblotting

Immunoblotting was performed as described previously [37]. Total cardiac cellular protein from mice (WT, Flotillin-1 KO mice, Flotillin-2 KO mice and Flotillin-1/2 KO mice) was blotted. For immunoblotting of siRNA experiments, ventricular NRCMs were plated on 24 wells plates and scraped 24 h after transfection. Cells were lysed in a stringent lysis buffer supplemented with protease inhibitors.

All protein samples were separated on a 10% (or 7% for Na_v1.5) SDS-PAGE gel, electro-transferred on nitrocellulose membranes and blocked with 5% milk powder or 5% bovine serum albumin. Equal efficiency of protein transfer was assessed by a Ponceau-S staining. Membranes were incubated with mouse monoclonal antibodies against pan-cadherin (Ncad, 1:10000, Sigma-Aldrich), DSG-2 (1:1000, Progen, Heidelberg, Germany), Plakophilin-2 (PKP2; 1:250, Progen), Plakoglobin (1:4000, Sigma-Aldrich), Desmocollin-2 (DSC-2; 1:500, Millipore, Temecula, CA, USA), Cx43 (1:250, BD Transduction) or Cx43 (1:250, Invitrogen, Camarillo, USA), and Na_v1.5 (1:250, Sigma-Aldrich), and rabbit polyclonal antibodies against Flotillin-1 (1:250, Sigma-Aldrich) and Flotillin-2 (1:250, Thermo Scientific). Secondary labeling was performed with an HRP-conjugated anti-mouse whole IgG antibody (1:7000, Jackson ImmunoResearch Laboratories Inc., Newmarket, United Kingdom) or an HRP-conjugated anti-rabbit whole IgG antibody (1:7000, BioRad Laboratories, Hercules, USA). Detection was performed using standard ECL procedure (Santa Cruz Biotechnology Inc., Heidelberg, Germany)

with ChemiDoc XRS system (BioRad Laboratories). Quantification analysis was performed using ImageJ 1.48v software (National Institutes of Health, USA), where the protein of interest was corrected for the corresponding area taken from the Ponceau-S staining.

2.5. Real-time quantitative PCR

Real-time quantitative PCR (RT-qPCR) on cardiac murine tissue was performed using TaqMan Gene Expression Assays (Applied Biosystems by Life Technologies Corp., Carlsbad, CA, USA) as described earlier [38]. Relative murine mRNA expression levels were determined for Flotillin-2, Flotillin-1, Collagen 1α1 (Col-1α1), Collagen 1α2 (Col-1α2), Collagen 3α1 (Col-3α1), brain natriuretic peptide (BNP), Ncad, Plakoglobin, DSP, DSG-2, Cx43, Na_v1.5 and L-type Ca-channel (all from Applied Biosystems by Life Technologies Corp., Carlsbad, USA). Geometric mean of GAPDH, Beta-2 microglobulin (B2m) and TATA-binding protein (Tbp) (Applied Biosystems) were used as internal controls, since the levels did not differ between group samples (for assay-IDs see Supplementary Table 1).

2.6. Histochemistry

To visualize cardiac fibrosis in murine hearts, 10 µm thick four-chamber-view cryo sections that were fixated in paraformaldehyde were stained with 0.1% Picrosirius Red solution, as described previously [39]. After staining, sections were digitally scanned using Aperio ScanScope XT (Leica Microsystems BV, Son, The Netherlands) and pictures were taken using NDPview2 (Hamamatsu Photonics KK, Shizuoka, Japan). The amount of fibrosis was determined using ImageJ 1.48v software (National Institutes of Health, USA), where the percentage of fibrosis was calculated as the fibrosis positive signal in the ventricles relative to the total ventricular surface area.

2.7. Co-immunoprecipitation of Flotillins

To investigate potential binding partners of Flotillins, co-immunoprecipitations (Co-IPs) were performed. Frozen murine hearts and human cardiac tissue were pulverized and incubated in IP-buffer (20 mM HEPES, 125 mM NaCl, 10% glycerol, 1 mM EDTA, 1 mM EGTA, 1 mM dithiothreitol, 1% Triton X-100 pH 7.6, freshly added 50 mM NaF, 1 mM Na₃VO₄, 1 mM PMSF and 1 µg/mL aprotinin from bovine lungs (Sigma-Aldrich) for 15 min at room temperature. Lysate was centrifuged for 10 min at 14.000 rpm and protein concentration was measured in the supernatant. Co-IP samples of 1 mg protein were first incubated (pre-cleared) with protein A- and G-agarose beads (Sigma-Aldrich) for one hour and centrifuged for 1 min at 1000 rpm. The centrifuged beads were used to generate pre-cleared samples in order to exclude that proteins would be able to bind to the beads without presence of any antibodies. The supernatant was distributed over two tubes and one part was incubated with 1 µg antibody (Flotillin-1 (Sigma-Aldrich) or Flotillin-2 (Cell Signaling Technology and Thermo Scientific)) for 2 h. The other part was incubated without primary antibodies in order to check, whether the secondary antibody could be able to a-specifically bind to the protein. Afterwards, protein A- and G-agarose beads were again added and incubated overnight. The next day, after centrifugation, the pellet was washed with IP-buffer and the supernatant was used for Immunoblotting.

2.8. Flotillin knockdown in NRCMs by siRNA transfection

Seventy-two hours after NRCM isolation, cells were transfected using Lipofectamine RNAiMAX (Thermo Fisher Scientific) with either 50 nM siRNA against Flotillin-1 (ID 64665) Trilencer-27 Rat siRNA (SR514199), Origene Technologies, Inc.), 20 nM siRNA against Flotillin-2 (ID 83764) Trilencer-27 Rat siRNA (SR 500907), Origene Technologies, Inc.) or both. Transfection with 10 nM scrambled siRNA (Trilencer-27 Universal Scrambled Negative Control siRNA duplex (SR 30004)) and non-transfected cells were used as controls. From every

experiment, a few wells were used to validate the efficiency of transfection by Western Blot (see Fig. 4A).

2.9. Patch clamp electrophysiology

NRCMs were plated on laminin-coated (Roche) cell culture dishes and transfected with siRNAs (scrambled or Flotillin1/2 KD). Peak inward sodium current (I_{Na}) measurements were performed 24 h post transfection as previously described using a HEKA EPC-10 USB amplifier (HEKA, Lambrecht, Germany) controlled by PatchMaster 2 × 90.2 [40]. Experiments were performed at 20 °C using a bath solution containing (in mmol/L): NMDG 140, KCl 4, CaCl₂ 1, MgCl₂ 1, glucose 6, NaHCO₃ 17.5, HEPES 15, pH 7.4/HCl. Pipette buffer contained CsCl 120, TEACl 10, MgCl₂ 3, CaCl₂ 1, Na₂ATP 2, EGTA 10, HEPES 5, pH 7.2/CsOH.

Peak current-voltage plots of individual recordings were fit with an equation describing sodium channel activation following the Hodgkin-Huxley formalism ($I(V) = G_{Na, max} * (V_m - E_{rev}) * 1 / (1 + \exp(-(-V_m - V_{half}) / Slope))^3$). Subsequently, parameters resulting from the fitting procedure ($G_{Na, max}$, E_{rev} , V_{half} and Slope) were compared between the group treated with scrambled siRNA and that with siRNA targeting Flotillin-1 and Flotillin-2. Fitting of current-voltage plots was done using Fitmaster 2 × 90.2.

2.10. Multi-electrode array (MEA) recordings

Electrical activity of the NRCM monolayers 96 h after plating (either transfected or not) was measured using laminin-coated 48-well MEA plates. Each well contained 16 nano-textured gold microelectrodes (~40–50 μm in diameter; 350 μm center-to-center spacing) with four integrated ground-electrodes, resulting in an array of 768 microelectrodes (Axion Biosystems Inc.). Before starting the recordings, cells were allowed to stabilize in the system for 5 min. Signals were recorded using a Maestro 768-channel amplifier with integrated heating system and temperature controller (constant temperature of 37 °C). Axion's Integrated Studio (AxIS Maestro v2.1) was used to manage data acquisition.

Raw data files on the spontaneously beating cardiomyocytes were recorded with Maestro acquisition settings with a sampling frequency of 12.5 kHz/channel using cardiac low amplitude settings (1200 × gain, 0.1–200 Hz band-pass filter).

Raw data files were re-recorded and spikes were detected using the AxIS spike detector with a minimum/maximum cycle length of 250 ms/5 s. Further analyses on cycle length (ms), spike amplitude (mV), spike slope (μV/s) and conduction velocities (cm/s) were performed on 30 consecutive beats per well of the re-recorded files. Activation maps were reconstructed from moments of activation for each electrode in all wells using Matlab2017b. Data from seven experiments were combined using a factor correction method as described in Ruijter et al. [41]

2.11. eQTL analysis of *Scn5a-1798insD*⁺ mice

We tested correlation between Flotillins and electrocardiogram measurements in a conduction disease-sensitized F2 mouse progeny obtained by intercrossing mice carrying the *Scn5a-1798insD*⁺ mutation from two separate genetic backgrounds (i.e. FVB/N and 129P2) for two generations [42]. Surface ECG parameters and left ventricular microarray data were available for 109 F2 mice, allowing for assessment of correlation between mRNA expression levels and conduction indices [43].

2.12. Statistics

Data are expressed as mean ± standard error of the mean (SEM). Statistical analyses were performed using appropriate parametric or non-parametric tests (students *t*-test or one-way ANOVA followed by Tukey's multiple comparisons test or Kruskal-Wallis followed by Dunn's multiple comparison test). All analyses were performed with GraphPad Prism 6.0 (GraphPad Software Inc., La Jolla, USA) or IBM SPSS Statistics for

Windows 20.0 (Chicago, USA). For eQTL analysis, transcripts were tested for correlations with the respective ECG indices. Spearman's correlation coefficients (rho) were generated with a commercial program IBM SPSS 16.0. A value of $p < .05$ was considered statistically significant.

3. Results

3.1. Flotillins are expressed in the heart and located in the cardiac intercalated disc

In a previous study, we confirmed the presence of Flotillin-2 in the ID of human and animal cardiac tissue, where it was significantly elevated in patients with DCM and ACM [5].

Fig. 1A shows that next to Flotillin-2, also Flotillin-1 is present in human and murine IDs where it substantially colocalizes with Ncad, as well as with Cx43 (Fig. 1B). Immuno precipitations confirmed that in murine and human cardiac tissue (of a control and an ACM patient), both Flotillins interact with each other (Fig. 1C, left panel for human tissue; right panel for murine tissue).

3.2. Flotillin deficiency reduces $Na_v1.5$ expression in absence of structural remodeling

Total KO of Flotillin-1, Flotillin-2 or both Flotillins in genetically engineered mice was confirmed by Western Blot and RT-qPCR (Fig. 2A and B, respectively). KO of Flotillin-1 caused a decrease in Flotillin-2 protein levels, and the inverse was also true for the Flotillin-2 KO mice (Fig. 2A). Though qPCR data suggest a similar trend, the slight reductions in mRNA were not significant (Fig. 2B).

No overt structural changes were seen in either Flotillin-1, Flotillin-2 or Flotillin double KO mice, and no increased fibrosis was detected by Sirius Red staining (Supplementary Fig. 1A and B). In line with that, mRNA levels of collagens were unchanged, except for Col-1α1, which was significantly increased in Flotillin-1/2 double KO mice, as compared to Flotillin-1 KO mice (Supplementary Fig. 1C). Furthermore, mRNA levels of the hypertrophic marker BNP were similar in all groups (Supplementary Fig. 1C).

Since Flotillins have previously been reported to influence Ncad, Plakoglobin and DSG-2 in epithelial cells, myoblasts or keratinocytes [20,34], we studied the consequences of Flotillin KO on their mRNA and protein levels. However, no significant changes in protein levels were seen in Ncad or Plakoglobin or their respective mRNA levels (Fig. 2C and D, respectively), with the exception of a significant increase of DSG-2 mRNA in Flotillin-1/2 KO mice, as compared to WT mice (Fig. 2D). Other ID proteins, such as PKP2 and DSC-2 were also unchanged (data not shown).

In addition, protein and mRNA levels of Cx43 and $Na_v1.5$ were evaluated. Protein levels of $Na_v1.5$ were significantly reduced in Flotillin-1 and Flotillin-1/2 KO mice compared to WT animals (Fig. 3A and B). Cx43 protein and Cx43 dephosphorylated at serine 368 (designated as Cx43NP), were not altered upon Flotillin KO (Fig. 3B), and mRNA levels of *Gja1* (Cx43) and *Scn5a* ($Na_v1.5$) were not changed (Fig. 3C). The observed decreased $Na_v1.5$ expression in Flotillin KO mice suggests a potential modulatory role of Flotillins in cardiac conduction. To explore this further, we made use of existing data from a previous study (see 2.11). This revealed a significant negative correlation between LV expression levels of Flotillin-1 and QRS-duration (probe 1: rho = -0.3446, $p = .00012$; probe 2: rho = -.1784, $p = .051$) was observed, but not between Flotillin-1 and heart rate, PR-interval, or QTc-duration. These findings suggest a modulatory effect of Flotillin-1 on cardiac electrical function, in particular ventricular conduction. Given these findings, we next investigated the functional consequences of Flotillin deficiency with respect to sodium channel function, conduction, and excitability. For that, NRCMs were transfected with siRNAs against Flotillin-1 and/or Flotillin-2 followed by patch clamp and MEA analysis.

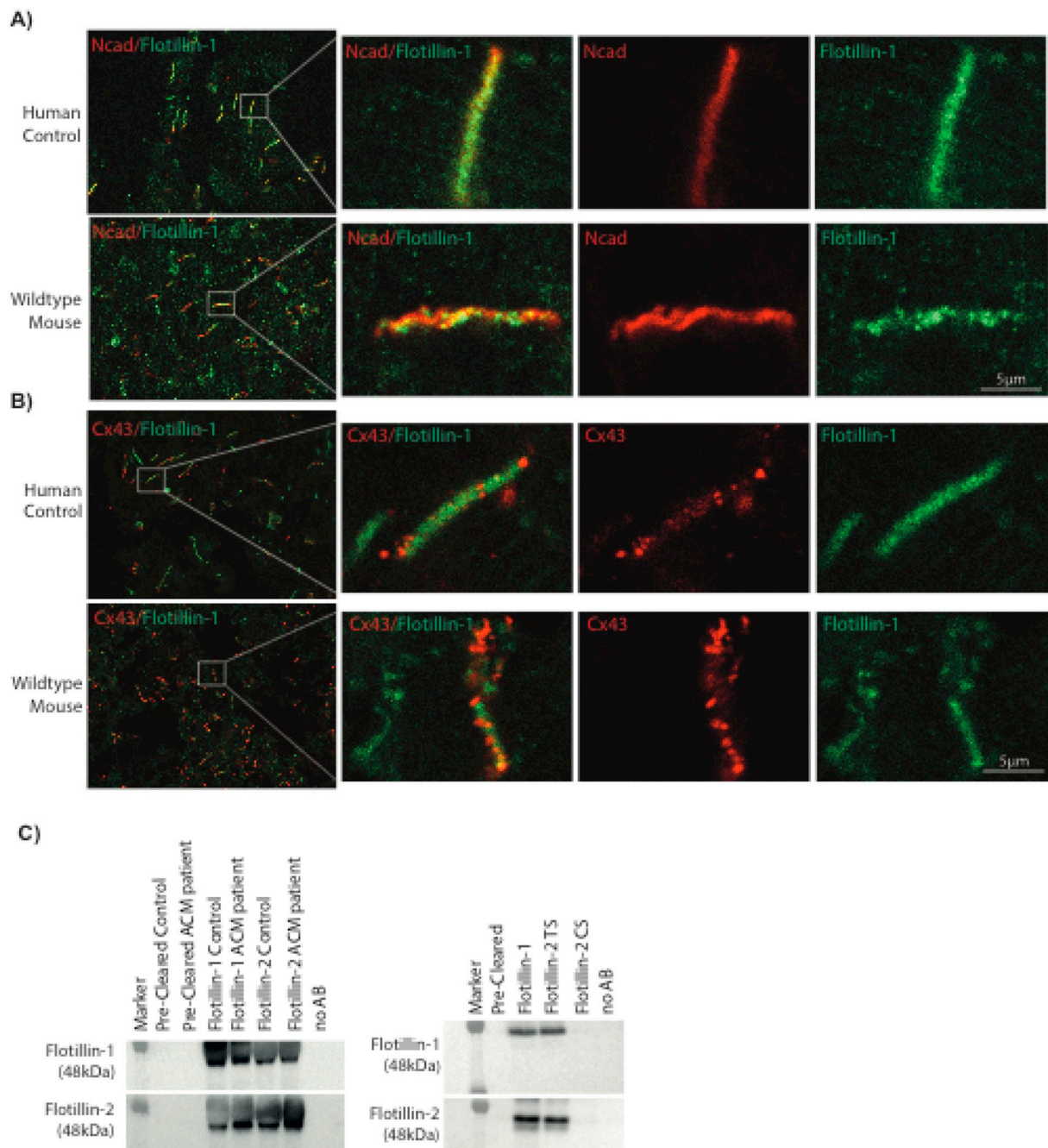


Fig. 1. Flotillins in the ID and in cardiac tissue before and after cardiac remodeling.

A) Representative images of N-Cadherin (Ncad; red) and Flotillin-1 (green) co-localization in human and murine control intercalated discs. B) Representative images of Connexin-43 (Cx43; red) and Flotillin-1 (green) co-localization in human and murine control intercalated discs. Left picture is taken with a 63 × objective. Other pictures are zoomed in on the white square indicated in the left pictures. C) Representative Western Blots of Co-immunoprecipitations on human tissue from a Control and an Arrhythmogenic Cardiomyopathy (ACM) patient (left panel) and murine tissue (right panel) for Flotillin-1 and Flotillin-2 using Flotillin-1 (Sigma) and Flotillin-2 (Thermo Scientific) antibodies to fish.

3.3. Functional consequences of Flotillin knockdown

To test the functional consequence of Flotillin KD on impulse propagation and excitability, NRCMs were transfected with siRNAs against Flotillin-1 or Flotillin-2 and functional measurements were performed. Treatment of NRCMs with siRNAs against Flotillin-1 or Flotillin-2, but not with scrambled siRNAs, resulted in a partial KD of both proteins (Fig. 4A). The knockdown of Flotillin-2 considerably reduced the amount of Flotillin-2, with a concomitant reduction of Flotillin-1. However, Flotillin-1 siRNA resulted in only a modest reduction of Flotillin-1

expression and a clear reduction in Flotillin-2. Double transfection of the siRNAs also resulted in a modest reduction of both Flotillins.

To establish effects on sodium channel function, patch clamp measurements were performed (Fig. 4B). Since $\text{Na}_v1.5$ protein levels were mainly reduced in Flotillin-1 and Flotillin-1/2 KO mice and spike amplitude was reduced in Flotillin-2 KD monolayers, these experiments were performed on scrambled and Flotillin-1/2 KD cells. Peak inward sodium current appeared to be significantly decreased in Flotillin-1/2 KD cells compared to scrambled cells (Fig. 4B) at test potentials between -20 and $+25$ mV. Fitting the current-voltage relationships of

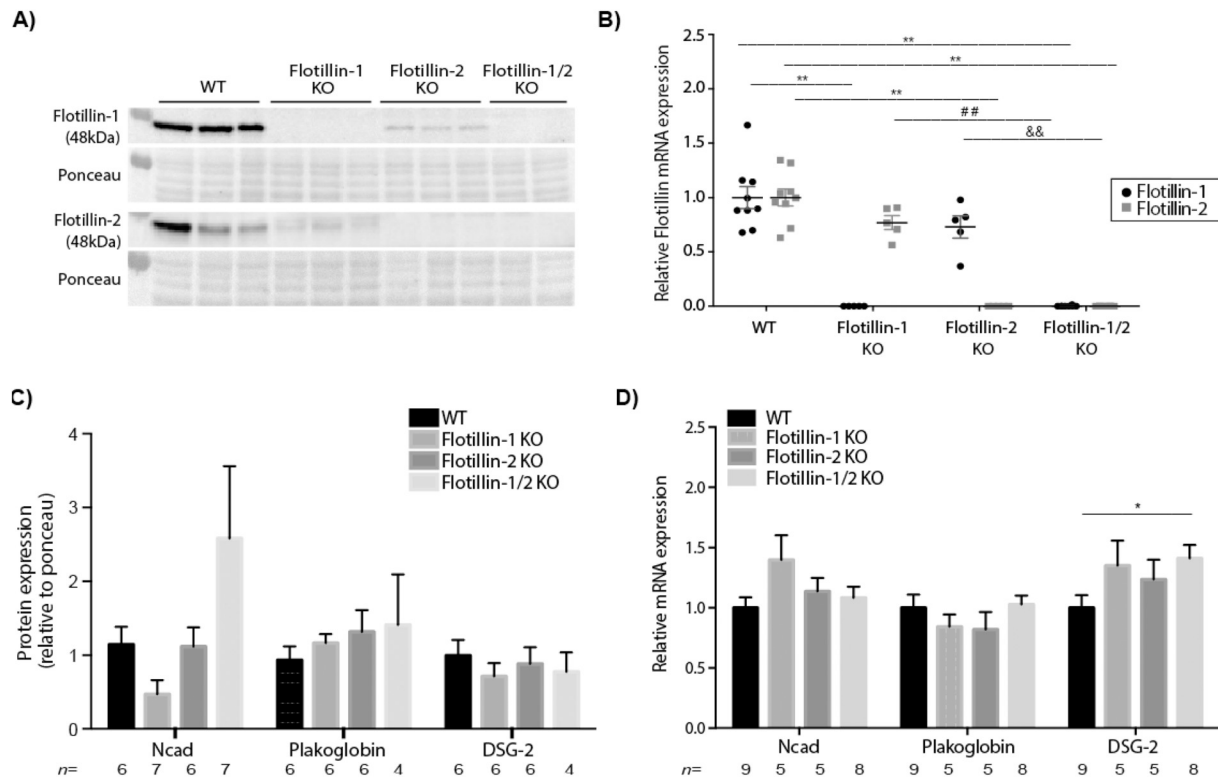


Fig. 2. Molecular ID changes upon Flotillin knockout in mice.

A) Representative Western Blot of Flotillin-1 and Flotillin-2 with respective Ponceau staining in wildtype (WT), Flotillin-1 knockout (KO), Flotillin-2 KO and Flotillin-1/2 KO mice. B) Relative mRNA expression of Flotillin-1 and Flotillin-2 assessed by RT-qPCR in WT, Flotillin-1 KO, Flotillin-2 KO and Flotillin-1/2 KO mice. C) Quantitative protein expression of N-Cadherin (Ncad), Plakoglobin and Desmoglein-2 (DSG-2) relative to Ponceau in WT, Flotillin-1 KO, Flotillin-2 KO and Flotillin-1/2 KO mice. D) Relative mRNA expression of Ncad, Plakoglobin and DSG-2 and Flotillin-2 assessed by RT-qPCR in WT, Flotillin-1 KO, Flotillin-2 KO and Flotillin-1/2 KO mice. *n* indicates the number of mice per group. * *p* < .05 and ** *p* < .01 compared to WT, ## *p* < .01 compared to Flotillin-1 KO and & *p* < .01 compared to Flotillin-2 KO.

individual cells confirmed reduced macroscopic sodium channel conductance ($G_{Na, \max}$ 582 ± 60 vs. $388 \pm 67 \text{ V}^{-1}$, scrambled and Flotillin-1/2 KD respectively, *p* < .05), but found no differences in reversal potential (E_{rev}), V_{half} or slope factor (see Table 1).

In order to assess potential effects on impulse propagation, MEA experiments were performed on control, scrambled, Flotillin-1 KD, Flotillin-2 KD and Flotillin 1/2 KD NRCMs. Supplementary Fig. 2 shows examples of field potentials recorded from 16 electrodes (left) and one electrode (right). Characteristics that could be extracted are the cycle length (s), spike amplitude (mV), slope of the signal ($\mu\text{V/s}$) and conduction velocity (cm/s). Field potentials are extracellularly recorded reflections of cellular action potentials fired within the context of the multicellular preparation. Spike slope showed a slight tendency to be decreased after KD of Flotillins as compared to control cells and scrambled cells (Fig. 4D). This was particularly seen after Flotillin-2 and -1/2 KD. Since the Flotillin-1 knockdown efficiency was only modest, it is not possible to conclude if Flotillin-1 ablation also would result in similar changes. Spike amplitude, which can be affected by several factors (including gap junctional coupling, monolayer geometry and cardiomyocyte excitability), was only significantly reduced after Flotillin-2 KD (Fig. 4E). Cycle length and conduction velocity were unchanged after siRNA treatment (Fig. 4C, F and G).

4. Discussion

Given their high evolutionary conservation, Flotillins are thought to have important cellular functions [44]. As mentioned earlier, Flotillins play, among others, a role in membrane trafficking, cell-to-cell coupling, adherens junction and desmosomal adhesion, and are involved in various forms of cancer [45].

We have previously shown for Flotillin-2 [5], and in this study for Flotillin-1 that they are present in the cardiac ID and bind to each other (Fig. 1A and B). Beyond this observation, their biological role within cardiomyocytes and their potential involvement in cardiac remodeling during disease has not yet been investigated. In our current study, we aimed at investigating the involvement of Flotillin-1 and Flotillin-2 in cardiac function with special attention to their potential role in electrophysiological characteristics.

Previously, it has been shown that Flotillin KO did not cause any phenotypical defects in drosophila, but Flotillin overexpression leads to disturbances in cell-to-cell adhesion molecules [18]. Also in the mouse hearts that we studied, no overt structural aberrancies could be detected, as the hearts were not hypertrophied, nor contained elevated levels of fibrosis (Supplementary Fig. 1). Although it has been shown that cadherin stabilization at the cell-to-cell junctions of myoblasts and breast cancer cells is Flotillin-dependent,²⁸ in our study, Flotillin KO did not seem to affect total Ncad protein and mRNA levels (Fig. 2C and D).

Moreover, Flotillins have been reported to stabilize Desmogleins at the cell-to-cell junctions, and it has been shown that loss of Flotillins causes weakening of desmosomal junctions in keratinocytes due to a more rapid turnover of Desmoglein-3 (DSG-3) [20]. In the heart, DSG-2 instead of DSG-3 is the main Desmoglein, but its protein levels were unchanged after Flotillin KO. Fluorescent immunohistochemistry for DSG-2 did not show differences in the localization between WT and KO mice (data not shown). On the other hand, previous studies have indicated that desmosomal dysfunction initiates cardiac remodeling and in particular dilated cardiomyopathy [46–48]. The fact that Flotillin-1, Flotillin-2 and double KO hearts did not show any structural alterations suggest that indeed desmosomal integrity at the ID was not profoundly impaired, or additional stressors are necessary to induce detectable

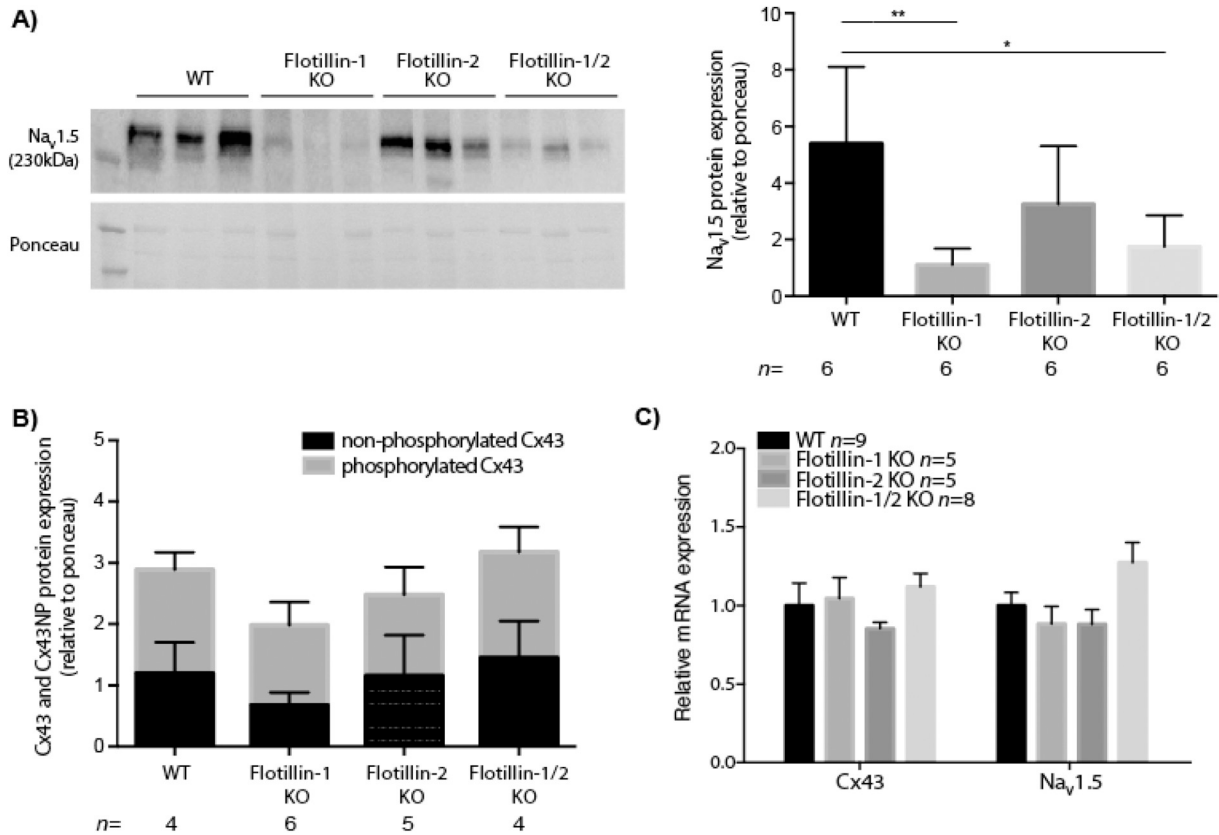


Fig. 3. Effect of Flotillin KO on Cx43 and $Na_v1.5$.

A) Representative Western Blot with respective Ponceau staining (left) and quantitative protein expression (right) of $Na_v1.5$ relative to Ponceau in WT, Flotillin-1 KO, Flotillin-2 KO and Flotillin-1/2 KO mice. B) Quantitative protein expression of Cx43 (grey bars) and Cx43NP (black bars) relative to Ponceau in WT, Flotillin-1 KO, Flotillin-2 KO and Flotillin-1/2 KO mice. C) Relative mRNA expression of Gja1 (Cx43) and Scn5a ($Na_v1.5$) assessed by RT-qPCR in WT, Flotillin-1 KO, Flotillin-2 KO and Flotillin-1/2 KO mice. n indicates the number of mice per group. * $p < .05$ and ** $p < .01$ compared to WT.

alterations. In line with that assumption, most other cardiac ID proteins seemed to be unaffected by the KO (Fig. 2C and D and Fig. 3B and C).

Interestingly, protein levels of the sodium channel $Na_v1.5$ were significantly reduced in Flotillin-1 and Flotillin-1/2 KO compared to WT mice (Fig. 3A), although mRNA levels were unchanged, suggesting that Flotillin-1 could be involved in trafficking of $Na_v1.5$ to, or recycling from the membrane rather than in transcriptional regulation. Changes in expression and functionality of $Na_v1.5$ leading to disturbances of the electrical excitability of cardiomyocytes are observed in various cardiac diseases, such as long QT syndrome, Brugada syndrome and ACM [49,50]. In a cohort of patients with ACM, but without any known mutations, we therefore searched for rare Flotillin variants and found one male patient (NYHA III, ejection fraction of 25%, persistent atrial fibrillation and recurrent ventricular tachyarrhythmia, no coronary artery disease, diabetes, stroke and implantable cardiac defibrillator received in 2010) with an exonic Flotillin-2 variant (p.L398M). Unfortunately, the patient had no siblings or family members to investigate, but his father died at the age of 36 years after hospitalization due to a cardiac event. This supports the hypothesis that Flotillins could modulate the integrity of the ID in disease, since ACM is considered a disease of the ID.

To investigate the effect of Flotillin reduction or absence on cardiac function, Flotillin KD was achieved in cultured NRCMs as depicted in Fig. 4A. To test whether sodium current density was reduced in Flotillin KD cells, patch clamp experiments were performed on these NRCMs. Although the KD in those cells was only partial in comparison to the total KO in the mouse models, still this Flotillin-1/2 KD resulted in a significantly decreased peak sodium current (Fig. 4B), which indicates that Flotillins are involved in regulating cardiac excitability. Moreover, Flotillin-2 and -1/2 KD resulted in a slight tendency of a reduction in field potential spike slope

(Fig. 4D) as compared to control and scrambled cells, which may suggest reduced cardiomyocyte excitability, but due to the multicellular nature of the preparation it is not possible to exclude alternative influences that can have similar effects on field potential morphology, such as gap junctional coupling and variations in culture geometry. Given the very modest KD of Flotillin-1, it is difficult to address whether Flotillin-1 is able to affect sodium channel function directly or whether the effects are primarily caused via the interplay between the two Flotillins.

Intriguingly, lipid rafts containing both Flotillins, $Na_v1.5$ and several potassium channels, are known to play a role in cell membrane excitability [51]. It has been hypothesized that $Na_v1.5$ in lipid rafts forms a reservoir for functional sodium channels and can be recruited when needed [52]. We may speculate that Flotillin KO or KD therefore hampers the recruitment of $Na_v1.5$ to these functional sodium channels, or even leads to its increased degradation. This is supported by the fact that we do not see changes in mRNA levels of $Na_v1.5$, but its protein levels are reduced and the excitability of NRCMs is altered.

Surprisingly, high levels of $Na_v1.5$ are found in cancer cells and the level of their expression and their activity is related to the aggressiveness of the cancer and the formation of metastases [53]. Interestingly, also Flotillin expression is increased in various forms of cancer, which could result in an upregulation of $Na_v1.5$ and in turn lead to more metastases [29–32]. In this study, we showed that Flotillin KO causes a decrease in $Na_v1.5$, which indeed provides fuel to speculate that $Na_v1.5$ levels might play a role in the Flotillin-induced effect on metastases.

Lastly, conduction velocity was not affected after Flotillin KD (Fig. 4F and G), in line with unaltered Cx43 mRNA and protein levels seen after KO in mice (Fig. 3B and C). Earlier studies have demonstrated that conduction velocity is maintained despite reduced sodium channel

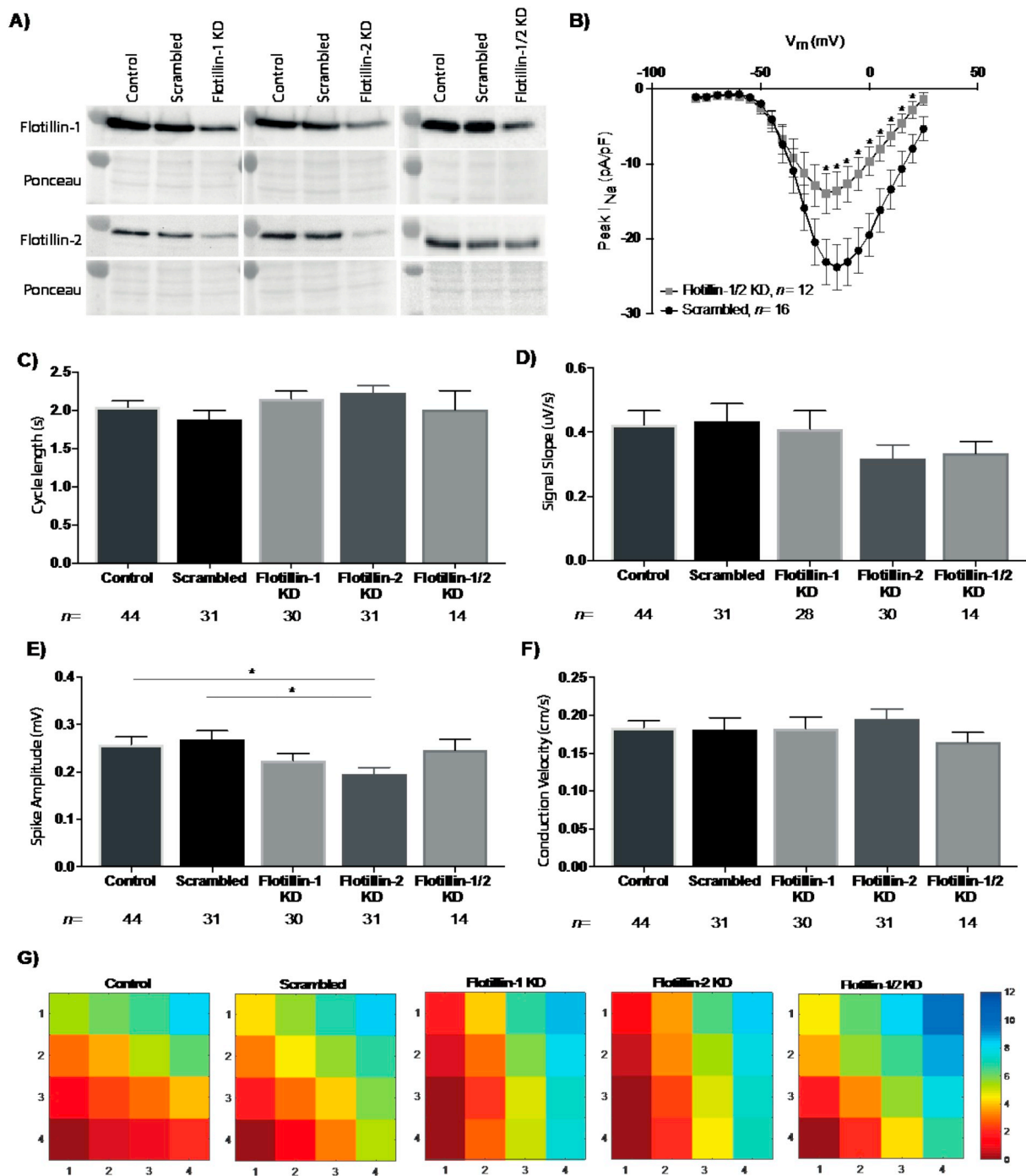


Fig. 4. Field potential changes upon Flotillin knockdown (KD) in Neonatal Rat Cardiomyocytes. A) Representative Western Blot of Flotillin-1 and Flotillin-2 with respective Ponceau staining in control, scrambled, Flotillin-1 knockdown (KD) and Flotillin-2 KD neonatal rat cardiomyocytes (NRCMs). B) Measured peak inward sodium current (pA/pF) in scrambled (circles) and Flotillin-1/2 KD (squares). C) Cycle length (s). D) Signal slope ($\mu V/s$). E) Signal amplitude (mV). F) Conduction velocity (cm/s). G) Representative activation maps measured by MEA. Colors represent the timepoint of activation. Earliest activation is depicted in red, latest in blue. Colour code is depicted on the right. *n* indicates the number of cells in B and wells in C–F per group. * $p < .05$ and ** $p < .01$. Numbers on the x-axis and y-axis in panel 4G refer to the electrode position.

function, [54–56] and that it only reduces when other factors contributing to conduction (reduced gap junctional coupling and enhanced fibrosis) are also affected. Although the relationship between Cx43 and $Na_v1.5$ has been shown in several studies, especially in combination with alterations in PKP2 [57–61], this does not seem to be of influence in the Flotillin KO mice or the siRNA treated cultured NRCMs in this current study. The fact that PKP2 and Cx43 were unchanged in the KO mice suggests that the reduction of $Na_v1.5$ and the resulting electrical

alterations are related to a different mechanism, possibly involving lipid rafts that contain Flotillins.

5. Conclusion

In this study, we have shown that Flotillins reside in the cardiac ID and bind to each other in murine and human cardiac tissue. Flotillin KO

Table 1

Sodium channel activation parameters of neonatal rat cardiomyocytes transfected with a scrambled siRNA or siRNAs against Flotillin-1 and Flotillin-2.

	Scrambled (n = 16)	Flotillin-1/2 KD (n = 10)	p value
V _{half} (mV)	-38.8 ± 2.4	-44.9 ± 2.0	0.085
Slope factor	7.7 ± 0.4 × 10 ⁻³	9.2 ± 0.7 × 10 ⁻³	0.062
G _{Na,max} (pS/pF)	582 ± 60	388 ± 67	0.047
E _{rev, Na} (mV)	31.2 ± 2.6	28.7 ± 3.1	0.545

and KD alter the levels of Na_v1.5 protein and the sodium current, without any obvious structural adaptations in KO mice. Thus, Flotillins seem to influence the functionality of Na_v1.5, and therefore also cardiac excitability, at least by modulation of the Na_v1.5 reserve or in an as yet undiscovered way. Finally, Flotillins may serve as potential candidate genes to investigate mutation-negative ACM patients.

Acknowledgements

Micaela Ebert, MD Department of Electrophysiology, Heart Center, University of Leipzig, Leipzig, Germany and Department of Cardiology, Leiden University Medical Center, Leiden, the Netherlands is acknowledged for patient inclusion.

Funding

We wish to acknowledge funding from the Netherlands Cardiovascular Research Initiative, an initiative supported by the Dutch Heart Foundation (CVON2012-10 PREDICT to ELK, LvS, JpVt, MAV, TABvV). RT and AB are supported by the German Research Council DFG Research Focus Unit FOR 2497 (Pegasus). IRE is supported by a Leducq Foundation network grant (RHYTHM).

Declarations of interest

None.

Appendix A. Supplementary data

Supplementary data to this article can be found online at <https://doi.org/10.1016/j.jmcc.2018.11.007>.

References

- M.S. Forbes, N. Sperelakis, Intercalated discs of mammalian heart: a review of structure and function, *Tissue Cell*. 17 (1985) 605–648.
- M. Noorman, M.A. van der Heyden, T.A. van Veen, M.G. Cox, R.N. Hauer, J.M. de Bakker, H.V. van Rijen, Cardiac cell-cell junctions in health and disease: electrical versus mechanical coupling, *J. Mol. Cell. Cardiol.* 47 (2009) 23–31, <https://doi.org/10.1016/j.jmcc.2009.03.016>.
- E.C. Beyer, D.L. Paul, D.A. Goodenough, Connexin43: a protein from rat heart homologous to a gap junction protein from liver, *J. Cell Biol.* 105 (1987) 2621–2629.
- S.H. Vermij, H. Abriel, T.A. van Veen, Refining the molecular organization of the cardiac intercalated disc, *Cardiovasc. Res.* (2017), <https://doi.org/10.1093/cvr/cvw259>.
- S. Soni, A.J. Raaijmakers, L.M. Raaijmakers, J.M. Damen, L. van Stuijvenberg, M.A. Vos, A.J. Heck, T.A. van Veen, A. Scholten, A proteomics approach to identify new putative cardiac intercalated disk proteins, *PLoS One* 11 (2016) e0152231, <https://doi.org/10.1371/journal.pone.0152231>.
- E. Rivera-Milla, C.A. Stuermer, E. Malaga-Trillo, Ancient origin of reggie (flotillin), reggie-like, and other lipid-raft proteins: convergent evolution of the SPFH domain, *Cell. Mol. Life Sci.* 63 (2006) 343–357, <https://doi.org/10.1007/s00018-005-5434-3>.
- M.F. Langhorst, A. Reuter, C.A. Stuermer, Scaffolding microdomains and beyond: the function of reggie/flotillin proteins, *Cell. Mol. Life Sci.* 62 (2005) 2228–2240, <https://doi.org/10.1007/s00018-005-5166-4>.
- G.P. Otto, B.J. Nichols, The roles of flotillin microdomains—endocytosis and beyond, *J. Cell Sci.* 124 (2011) 3933–3940, <https://doi.org/10.1242/jcs.092015>.
- G.P. Solis, M. Hoegg, C. Munderloh, Y. Schrock, E. Malaga-Trillo, E. Rivera-Milla, C.A. Stuermer, Reggie/flotillin proteins are organized into stable tetramers in membrane microdomains, *Biochem. J.* 403 (2007) 313–322, <https://doi.org/10.1042/BJ20061686>.
- A. Santamaria, E. Castellanos, V. Gomez, P. Benedit, J. Renau-Piqueras, J. Morote, J. Reventos, T.M. Thomson, R. Paciucci, PTOV1 enables the nuclear translocation and mitogenic activity of flotillin-1, a major protein of lipid rafts, *Mol. Cell. Biol.* 25 (2005) 1900–1911, <https://doi.org/10.1128/MCB.25.5.1900-1911.2005>.
- M. Bauer, L. Pelkmans, A new paradigm for membrane-organizing and -shaping scaffolds, *FEBS Lett.* 580 (2006) 5559–5564, <https://doi.org/10.1016/j.febslet.2006.08.077>.
- J. Liu, S.M. Deyoung, M. Zhang, L.H. Dold, A.R. Saltiel, The stomatin/prohibitin/flotillin/Hflk/C domain of flotillin-1 contains distinct sequences that direct plasma membrane localization and protein interactions in 3T3-L1 adipocytes, *J. Biol. Chem.* 280 (2005) 16125–16134, <https://doi.org/10.1074/jbc.M500940200>.
- I. Gkantiras, B. Brugger, E. Stuken, D. Kaloyanova, X.Y. Li, K. Lohr, F. Lottspeich, F.T. Wieland, J.B. Helms, Sphingomyelin-enriched microdomains at the Golgi complex, *Mol. Biol. Cell* 12 (2001) 1819–1833.
- C. Neumann-Giesen, B. Falkenbach, P. Beicht, S. Claasen, G. Luers, C.A. Stuermer, V. Tikkanen, Membrane and raft association of reggie-1/flotillin-2: role of myristoylation, palmitoylation and oligomerization and induction of filopodia by overexpression, *Biochem. J.* 378 (2004) 509–518, <https://doi.org/10.1042/BJ20031100>.
- M. Frick, N.A. Bright, K. Riento, A. Bray, C. Merrified, B.J. Nichols, Coassembly of flotillins induces formation of membrane microdomains, membrane curvature, and vesicle budding, *Curr. Biol.* 17 (2007) 1151–1156, <https://doi.org/10.1016/j.cub.2007.05.078>.
- T. Babuke, M. Ruonala, M. Meister, M. Amaddii, C. Genzler, A. Esposito, R. Tikkanen, Hetero-oligomerization of reggie-1/flotillin-2 and reggie-2/flotillin-1 is required for their endocytosis, *Cell. Signal.* 21 (2009) 1287–1297, <https://doi.org/10.1016/j.cellsig.2009.03.012>.
- C. Neumann-Giesen, I. Fernow, M. Amaddii, R. Tikkanen, Role of EGF-induced tyrosine phosphorylation of reggie-1/flotillin-2 in cell spreading and signaling to the actin cytoskeleton, *J. Cell Sci.* 120 (2007) 395–406, <https://doi.org/10.1242/jcs.03336>.
- M. Hoehne, H.G. de Couet, C.A. Stuermer, K.F. Fischbach, Loss- and gain-of-function analysis of the lipid raft proteins Reggie/Flotillin in Drosophila: they are posttranslationally regulated, and misexpression interferes with wing and eye development, *Mol. Cell. Neurosci.* 30 (2005) 326–338, <https://doi.org/10.1016/j.mcn.2005.07.007>.
- A. Banning, T. Babuke, N. Kurrle, M. Meister, M.O. Ruonala, R. Tikkanen, Flotillins regulate focal adhesions by interacting with alpha-actinin and by influencing the activation of focal adhesion kinase, *Cell* 7 (2018), <https://doi.org/10.3390/cells7040028>.
- F. Vollner, J. Ali, N. Kurrle, Y. Exner, R. Eming, M. Hertl, A. Banning, R. Tikkanen, Loss of flotillin expression results in weakened desmosomal adhesion and Pemphigus vulgaris-like localisation of desmoglein-3 in human keratinocytes, *Sci. Rep.* 6 (2016) 28820, <https://doi.org/10.1038/srep28820>.
- N. Hulsbusch, G.P. Solis, V.L. Katanaev, C.A. Stuermer, Reggie-1/Flotillin-2 regulates integrin trafficking and focal adhesion turnover via Rab11a, *Eur. J. Cell Biol.* 94 (2015) 531–545, <https://doi.org/10.1016/j.ejcb.2015.07.003>.
- C. Munderloh, G.P. Solis, V. Bodrikov, F.A. Jaeger, M. Wiechers, E. Malaga-Trillo, C.A. Stuermer, Reggies/flotillins regulate retinal axon regeneration in the zebrafish optic nerve and differentiation of hippocampal and N2a neurons, *J. Neurosci.* 29 (2009) 6607–6615, <https://doi.org/10.1523/JNEUROSCI.0870-09.2009>.
- E. Guillaume, F. Comunale, N. Do Khoa, D. Planchon, S. Bodin, C. Gauthier-Rouviere, Flotillin microdomains stabilize cadherins at cell-cell junctions, *J. Cell Sci.* 126 (2013) 5293–5304, <https://doi.org/10.1242/jcs.133975>.
- S. Bodin, D. Planchon, E. Rios Morris, F. Comunale, C. Gauthier-Rouviere, Flotillins in intercellular adhesion - from cellular physiology to human diseases, *J. Cell Sci.* 127 (2014) 5139–5147, <https://doi.org/10.1242/jcs.159764>.
- N. Kurrle, W. Ockenga, M. Meister, F. Vollner, S. Kuhne, B.A. John, A. Banning, R. Tikkanen, Phosphatidylinositol 3-Kinase dependent upregulation of the epidermal growth factor receptor upon Flotillin-1 depletion in breast cancer cells, *BMC Cancer* 13 (2013) 575, <https://doi.org/10.1186/1471-2407-13-575>.
- A. Banning, W. Ockenga, F. Finger, P. Siebrasse, R. Tikkanen, Transcriptional regulation of flotillins by the extracellularly regulated kinases and retinoid X receptor complexes, *PLoS One* 7 (2012) e45514, <https://doi.org/10.1371/journal.pone.0045514>.
- A. Banning, C.R. Regenbrecht, R. Tikkanen, Increased activity of mitogen activated protein kinase pathway in flotillin-2 knockout mouse model, *Cell. Signal.* 26 (2014) 198–207, <https://doi.org/10.1016/j.cellsig.2013.11.001>.
- J. Liu, W. Huang, C. Ren, Q. Wen, W. Liu, X. Yang, L. Wang, B. Zhu, L. Zeng, X. Feng, C. Zhang, H. Chen, W. Jia, L. Zhang, X. Xia, Y. Chen, Flotillin-2 promotes metastasis of nasopharyngeal carcinoma by activating NF-kappaB and PI3K/Akt3 signaling pathways, *Sci Rep.* 5 (2015) 11614, <https://doi.org/10.1038/srep11614>.
- M. Koh, H.Y. Yong, E.S. Kim, H. Son, Y.R. Jeon, J.S. Hwang, M.O. Kim, Y. Cha, W.S. Choi, D.Y. Noh, K.M. Lee, K.B. Kim, J.S. Lee, H.J. Kim, H. Kim, H.H. Kim, E.J. Kim, S.Y. Park, H.S. Kim, W.K. Moon, H.R. Choi Kim, A. Moon, A novel role for flotillin-1 in H-Ras-regulated breast cancer aggressiveness, *Int. J. Cancer* 138 (2016) 1232–1245, <https://doi.org/10.1002/ijc.29869>.
- S. Cao, Y. Cui, H. Xiao, M. Mai, C. Wang, S. Xie, J. Yang, S. Wu, J. Li, L. Song, X. Guo, C. Lin, Upregulation of flotillin-1 promotes invasion and metastasis by activating TGF-beta signaling in nasopharyngeal carcinoma, *Oncotarget* 7 (2016) 4252–4264, <https://doi.org/10.18632/oncotarget.6483>.
- Z. Li, Y. Yang, Y. Gao, X. Wu, X. Yang, Y. Zhu, H. Yang, L. Wu, C. Yang, L. Song, Elevated expression of flotillin-1 is associated with lymph node metastasis and poor prognosis in early-stage cervical cancer, *Am. J. Cancer Res.* 6 (2016) 38–50.
- T. Berger, T. Ueda, E. Arpaia, I.I. Chio, E.A. Shirdel, I. Jurisica, K. Hamada, A. You-

- Ten, J. Haight, A. Wakeham, C.C. Cheung, T.W. Mak, Flotillin-2 deficiency leads to reduced lung metastases in a mouse breast cancer model, *Oncogene* 32 (2013) 4989–4994, <https://doi.org/10.1038/onc.2012.499>.
- [33] G.P. Solis, Y. Schrock, N. Hulsbusch, M. Wiechers, H. Plattner, C.A. Stuermer, Reggins/flotillins regulate E-cadherin-mediated cell contact formation by affecting EGFR trafficking, *Mol. Biol. Cell* 23 (2012) 1812–1825, <https://doi.org/10.1091/mbc.E11-12-1006>.
- [34] N. Kurrle, F. Vollner, R. Eming, M. Hertl, A. Banning, R. Tikkanen, Flotillins directly interact with gamma-catenin and regulate epithelial cell-cell adhesion, *PLoS One* 8 (2013) e84393, <https://doi.org/10.1371/journal.pone.0084393>.
- [35] A.S. Yap, G.A. Gomez, R.G. Parton, Adherens Junctions Revisualized: Organizing Cadherins as Nanoassemblies, *Dev. Cell* 35 (2015) 12–20, <https://doi.org/10.1016/j.devcel.2015.09.012>.
- [36] A. Ludwig, G.P. Otto, K. Riento, E. Hams, P.G. Fallon, B.J. Nichols, Flotillin microdomains interact with the cortical cytoskeleton to control uropod formation and neutrophil recruitment, *J. Cell Biol.* 191 (2010) 771–781, <https://doi.org/10.1083/jcb.201005140>.
- [37] T.A. van Veen, H.V. van Rijen, R.F. Wiegner, T. Opthof, M.C. Colbert, S. Clement, J.M. de Bakker, H.J. Jongasma, Remodeling of gap junctions in mouse hearts hypertrophied by forced retinoic acid signaling, *J. Mol. Cell. Cardiol.* 34 (2002) 1411–1423.
- [38] M.S. Fontes, A.J. Raaijmakers, T. van Doorn, B. Kok, S. Nieuwenhuis, R. van der Nagel, M.A. Vos, T.P. de Boer, H.V. van Rijen, M.F. Bierhuizen, Changes in Cx43 and Nav1.5 expression precede the occurrence of substantial fibrosis in calcineurin-induced murine cardiac hypertrophy, *PLoS One* 9 (2014) e87226, <https://doi.org/10.1371/journal.pone.0087226>.
- [39] M.S. Fontes, E.L. Kessler, L. van Stuijvenberg, M.A. Brans, L.L. Falke, B. Kok, A. Leask, H.V. van Rijen, M.A. Vos, R. Goldschmeding, T.A. van Veen, CTGF knockout does not affect cardiac hypertrophy and fibrosis formation upon chronic pressure overload, *J. Mol. Cell. Cardiol.* 88 (2015) 82–90, <https://doi.org/10.1016/j.yjmcc.2015.09.015>.
- [40] M.K. Jonsson, M.A. Vos, G.R. Mirams, G. Duker, P. Sartipy, T.P. de Boer, T.A. van Veen, Application of human stem cell-derived cardiomyocytes in safety pharmacology requires caution beyond hERG, *J. Mol. Cell. Cardiol.* 52 (2012) 998–1008, <https://doi.org/10.1016/j.yjmcc.2012.02.002>.
- [41] J.M. Ruijter, A. Ruiz Villalba, J. Hellemans, A. Untergasser, M.J. van den Hoff, Removal of between-run variation in a multi-plate qPCR experiment, *Biomol Detect Quantif.* 5 (2015) 10–14, <https://doi.org/10.1016/j.bdq.2015.07.001>.
- [42] B.P. Scicluna, M.W. Tanck, C.A. Remme, L. Beekman, R. Coronel, A.A. Wilde, C.R. Bezzina, Quantitative trait loci for electrocardiographic parameters and arrhythmia in the mouse, *J. Mol. Cell. Cardiol.* 50 (2011) 380–389, <https://doi.org/10.1016/j.yjmcc.2010.09.009>.
- [43] E.M. Lodder, B.P. Scicluna, A. Milano, A.Y. Sun, H. Tang, C.A. Remme, P.D. Moerland, M.W. Tanck, G.S. Pitt, D.A. Marchuk, C.R. Bezzina, Dissection of a quantitative trait locus for PR interval duration identifies Tnni3k as a novel modulator of cardiac conduction, *PLoS Genet.* 8 (2012) e1003113, <https://doi.org/10.1371/journal.pgen.1003113>.
- [44] C.A. Stuermer, The reggie/flotillin connection to growth, *Trends Cell Biol.* 20 (2010) 6–13, <https://doi.org/10.1016/j.tcb.2009.10.003>.
- [45] T. Babuke, R. Tikkanen, Dissecting the molecular function of reggie/flotillin proteins, *Eur. J. Cell Biol.* 86 (2007) 525–532, <https://doi.org/10.1016/j.ejcb.2007.03.003>.
- [46] M. Pluess, G. Daeubler, C.G. Dos Remedios, E. Ehler, Adaptations of cytoarchitecture in human dilated cardiomyopathy, *Biophys. Rev.* 7 (2015) 25–32, <https://doi.org/10.1007/s12551-014-0146-2>.
- [47] H. Kitamura, Y. Ohnishi, A. Yoshida, K. Okajima, H. Azumi, A. Ishida, E.J. Galeano, S. Kubo, Y. Hayashi, H. Itoh, M. Yokoyama, Heterogeneous loss of connexin43 protein in nonischemic dilated cardiomyopathy with ventricular tachycardia, *J. Cardiovasc. Electrophysiol.* 13 (2002) 865–870.
- [48] R. Parvari, A. Levitas, The mutations associated with dilated cardiomyopathy, *Biochem. Res. Int.* 2012 (2012) 639250, <https://doi.org/10.1155/2012/639250>.
- [49] D. Shy, L. Gillet, H. Abriel, Cardiac sodium channel Nav1.5 distribution in myocytes via interacting proteins: the multiple pool model, *Biochim. Biophys. Acta* 1833 (2013) 886–894, <https://doi.org/10.1016/j.bbamcr.2012.10.026>.
- [50] L. Gillet, D. Shy, H. Abriel, Nav1.5 and interacting proteins in human arrhythmic cardiomyopathy, *Futur. Cardiol.* 9 (2013) 467–470, <https://doi.org/10.2217/fca.13.38>.
- [51] L. Brisson, L. Gillet, S. Calaghan, P. Besson, J.Y. Le Guennec, S. Roger, J. Gore, Na (V)1.5 enhances breast cancer cell invasiveness by increasing NHE1-dependent H (+) efflux in caveolae, *Oncogene* 30 (2011) 2070–2076, <https://doi.org/10.1038/onc.2010.574>.
- [52] A. Maguy, T.E. Hebert, S. Nattel, Involvement of lipid rafts and caveolae in cardiac ion channel function, *Cardiovasc. Res.* 69 (2006) 798–807, <https://doi.org/10.1016/j.cardiores.2005.11.013>.
- [53] P. Besson, V. Driffort, E. Bon, F. Gradek, S. Chevalier, S. Roger, How do voltage-gated sodium channels enhance migration and invasiveness in cancer cells? *Biochim. Biophys. Acta* 1848 (2015) 2493–2501, <https://doi.org/10.1016/j.bbamem.2015.04.013>.
- [54] T.A. van Veen, M. Stein, A. Royer, K. Le Quang, F. Charpentier, W.H. Colledge, C.L. Huang, R. Wilders, A.A. Grace, D. Escande, J.M. de Bakker, H.V. van Rijen, Impaired impulse propagation in Scn5a-knockout mice: combined contribution of excitability, connexin expression, and tissue architecture in relation to aging, *Circulation* 112 (2005) 1927–1935, <https://doi.org/10.1161/CIRCULATIONAHA.105.539072>.
- [55] C.A. Remme, A.O. Verkerk, D. Nuyens, A.C. van Ginneken, S. van Brunschot, C.N. Belterman, R. Wilders, M.A. van Roon, H.L. Tan, A.A. Wilde, P. Carmeliet, J.M. de Bakker, M.W. Veldkamp, C.R. Bezzina, Overlap syndrome of cardiac sodium channel disease in mice carrying the equivalent mutation of human SCN5A-1795insD, *Circulation* 114 (2006) 2584–2594, <https://doi.org/10.1161/CIRCULATIONAHA.106.653949>.
- [56] M. Stein, T.A. van Veen, C.A. Remme, M. Boulaksil, M. Noorman, L. van Stuijvenberg, R. van der Nagel, C.R. Bezzina, R.N. Hauer, J.M. de Bakker, H.V. van Rijen, Combined reduction of intercellular coupling and membrane excitability differentially affects transverse and longitudinal cardiac conduction, *Cardiovasc. Res.* 83 (2009) 52–60, <https://doi.org/10.1093/cvr/cvp124>.
- [57] J.A. Jansen, M. Noorman, H. Musa, M. Stein, S. de Jong, R. van der Nagel, T.J. Hund, P.J. Mohler, M.A. Vos, T.A. van Veen, J.M. de Bakker, M. Delmar, H.V. van Rijen, Reduced heterogeneous expression of Cx43 results in decreased Nav1.5 expression and reduced sodium current that accounts for arrhythmia vulnerability in conditional Cx43 knockout mice, *Heart Rhythm.* 9 (2012) 600–607, <https://doi.org/10.1016/j.hrthm.2011.11.025>.
- [58] M. Cerrone, X. Lin, M. Zhang, E. Agullo-Pascual, A. Pfenniger, H. Chkourko Gusky, V. Novelli, C. Kim, T. Tirasawadichai, D.P. Judge, E. Rothenberg, H.S. Chen, C. Napolitano, S.G. Priori, M. Delmar, Missense mutations in plakophilin-2 cause sodium current deficit and associate with a Brugada syndrome phenotype, *Circulation* 129 (2014) 1092–1103, <https://doi.org/10.1161/CIRCULATIONAHA.113.003077>.
- [59] P.Y. Sato, H. Musa, W. Coombs, G. Guerrero-Serna, G.A. Patino, S.M. Taffet, L.L. Isom, M. Delmar, Loss of plakophilin-2 expression leads to decreased sodium current and slower conduction velocity in cultured cardiac myocytes, *Circ. Res.* 105 (2009) 523–526, <https://doi.org/10.1161/CIRCRESAHA.109.201418>.
- [60] P.Y. Sato, W. Coombs, X. Lin, O. Nekrasova, K.J. Green, L.L. Isom, S.M. Taffet, M. Delmar, Interactions between ankyrin-G, Plakophilin-2, and Connexin43 at the cardiac intercalated disc, *Circ. Res.* 109 (2011) 193–201, <https://doi.org/10.1161/CIRCRESAHA.111.247023>.
- [61] M. Cerrone, M. Noorman, X. Lin, H. Chkourko, F.X. Liang, R. van der Nagel, T. Hund, W. Birchmeier, P. Mohler, T.A. van Veen, H.V. van Rijen, M. Delmar, Sodium current deficit and arrhythmogenesis in a murine model of plakophilin-2 haploinsufficiency, *Cardiovasc. Res.* 95 (2012) 460–468, <https://doi.org/10.1093/cvr/cvs218>.